

Multi-Label Activity Recognition using Activity-specific Features

Yanyi Zhang,¹ Xinyu Li,² Ivan Marsic¹

¹ Rutgers University New Brunswick, Electrical and Computer Engineering Department

² Amazon Web Service

yz593@scarletmail.rutgers.edu, xxnl@amazon.com, marsic@rutgers.edu

Abstract

We introduce an approach to multi-label activity recognition by extracting independent feature descriptors for each activity. Our approach first extracts a set of independent feature snippets, focused on different spatio-temporal regions of a video, that we call “observations”. We then generate independent feature descriptors for each activity, that we call “activity-specific features” by combining these observations with attention, and further make action prediction based on these activity-specific features. This structure can be trained end-to-end and plugged into any existing network structures for video classification. Our method outperformed state-of-the-art approaches on three multi-label activity recognition datasets. We also evaluated the method and achieved state-of-the-art performance on two single-activity recognition datasets to show the generalizability of our approach. Furthermore, to better understand the activity-specific features that the system generates, we visualized these activity-specific features in the Charades dataset.

Introduction

Activity recognition has been studied in recent years due to its great potential in real-world applications. Recent activity recognition researches (Kay et al. 2017; Soomro, Zamir, and Shah 2012; Goyal et al. 2017; Kuehne et al. 2011) focused on single-activity recognition assuming that each video contains only one activity, without considering a multi-label problem where each video may contain multiple activities (simultaneous or sequential), which has more general real-world use cases (e.g., sports activity recognition (Sozykin et al. 2018; Carboneau et al. 2015), or daily life activity recognition (Sigurdsson et al. 2016)). Most of the recent multi-label activity recognition methods are derived from structures for single-activity that generating a shared feature vector using the 3D average pooling and applying sigmoid as the output activation function (Li et al. 2017; Wang et al. 2016; Carreira and Zisserman 2017; Wang et al. 2018; Feichtenhofer et al. 2019; Wu et al. 2019). Although these approaches enable the network to provide multi-label outputs, the features are not representative of multi-label activities. These methods work well on single-activity recognition with the assumption that the learned feature maps will only activate on one region where the corresponding activity occurred. The remaining regions are considered as unrelated,

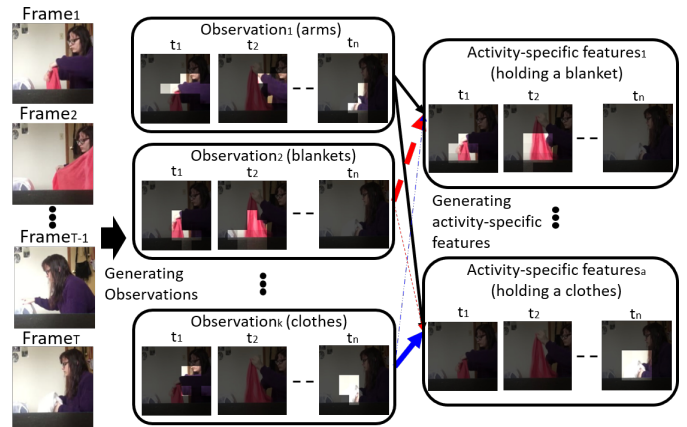


Figure 1: System overview using an example from Charades. The system first generates k independent feature snippets (“observations”) that focus on different key regions from the video (arms, blankets, and clothes). The activity-specific features are then generated by independently combining these observations. The weights of the observations that contribute to activity-specific features are represented as lines with different colors (black, red, and blue). The thicker lines denote higher weights. For example, the *Activity-specific features*₁ (holding a blanket) are obtained by combining information from *observation*₁ (focuses on arms) and *observation*₂ (focuses on clothes). More examples and detailed explanations are given in Figure 4.

and have low values in the feature maps. As a result, averaging feature maps over spatio-temporal dimension may represent single-activity features well. However, in multi-label activity videos, the feature maps may focus on multiple disconnected regions corresponding to the performed activities, and the 3D average pooling will globally merge the feature maps and make the rendered features unrepresentative.

To better represent multi-label activities performed in a video, we introduce our novel mechanism that generates independent feature descriptors for different activities. We named these feature descriptors “**activity-specific features**”. The introduced mechanism generates activity-specific features in two stages. The first-stage (Figure 1, middle) network summarizes the feature maps extracted by the backbone network (3D convolution layers) and generates a set of independent feature snippets by applying independent spatio-temporal attention for each snippet. We name these feature snippets “**observations**”. In the second stage

(Figure 1, right), the network then learns activity-specific features from different combinations of observations for different activities. In this way, each activity is represented as an independent set of feature descriptors (activity-specific features). The multi-label activity predictions can be then made based on the activity-specific features. Unlike most of the previous approaches (Li et al. 2017; Wang et al. 2016; Carreira and Zisserman 2017; Wang et al. 2018; Feichtenhofer et al. 2019; Wu et al. 2019) that generate a shared feature vector to represent multiple activities by pooling feature maps globally, our network produces specific feature descriptors for each activity, which is more representative. In multi-label activity videos, different activities might have different duration and need to be recognized using video clips with different lengths. To address this issue, we further introduced a **speed-invariant tuning** method for generating activity-specific features and recognizing multi-label activities using inputs with different downsampling rates. Our experimental results show that the network using the speed-invariant tuning method boosts around 1% mAP (mean average precision) score on Charades (Sigurdsson et al. 2016).

We compared our system with current state-of-the-art methods on three multi-label activity recognition datasets, a large-scale dataset, Charades (Sigurdsson et al. 2016) for the main experiment, and two other small multi-label sport activity datasets, Volleyball (Sozykin et al. 2018) and Hockey (Carbonneau et al. 2015). We also evaluated our method on Kinetics-400 (Kay et al. 2017) and UCF-101 (Soomro, Zamir, and Shah 2012) for single-activity recognition to show generalizability of our method. We outperformed the current state-of-the-art methods on all three multi-label activity recognition datasets by only using RGB videos as input (Feichtenhofer 2020; Sozykin et al. 2018; Azar et al. 2019). Our experimental results demonstrate that our approach for generating activity-specific features succeeds in multi-label activity recognition. We achieved similar performance with most recent state-of-the-art approaches (Feichtenhofer et al. 2019; Tran et al. 2019; Feichtenhofer 2020) on Kinetics-400 and UCF-101, which shows that our system, although focused on multi-label activity recognition, is able to achieve state-of-the-art performance on single-activity recognition datasets. We further visualized the activity-specific features by applying the learned attention maps on the backbone features (feature maps after the last 3D convolution layer) to represent the activity-specific feature maps. Our contributions can be summarized as:

1. A novel network structure that generates activity-specific features for multi-label activity recognition.
2. The speed-invariant tuning method that produces multi-label activity predictions using different temporal-resolution inputs.
3. We evaluated our method on five activity recognition datasets, including multi-label and single-activity datasets to show the generalizability of our method as well as produce an ablation study for selecting the parameters.

Related Work

Activity Recognition. Video-based activity recognition has been developing rapidly in recent years due to the success of deep learning methods for image recognition (Krizhevsky, Sutskever, and Hinton 2012; Szegedy et al. 2015; He et al. 2016). Compared to image classification, activity recognition depends on spatio-temporal features extracted from consecutive frames instead of spatio-only features from static images. Two-stream networks apply two-branch convolution layers to extract motion features from consecutive frames as well as spatial features from static images and fuse them for activity recognition (Simonyan and Zisserman 2014; Feichtenhofer, Pinz, and Zisserman 2016; Wang et al. 2016). Others proposed 3D-convolution-based networks for extracting spatio-temporal features from the videos instead of using manually designed optical flow for extracting motions between frames (Carreira and Zisserman 2017; Tran et al. 2015). The nonlocal neural network (Wang et al. 2018) and the long-term feature bank (LFB) (Wu et al. 2019) extended the 3D ConvNet by extracting long-range features. The SlowFast network (Feichtenhofer et al. 2019) introduced a two-pathway network for learning motion and spatial features separately from the videos. The most recent X3D network introduced an efficient video network that expands 2D networks from multiple axes (Feichtenhofer 2020). These methods work well on single-activity recognition datasets that achieved around 80% accuracy score on Kinetics-400 (Kay et al. 2017).

Multi-label Activity Recognition. Multi-label activity recognition is designed for recognizing multiple activities that are performed simultaneously or sequentially in each video. Most of the recent approaches focus on single-activity recognition by assuming that only one activity was performed in a video and produce the multi-label output by modifying the activation function from softmax to sigmoid when applied on multi-label activity datasets (Wang et al. 2016; Carreira and Zisserman 2017; Wang et al. 2018; Feichtenhofer et al. 2019; Wu et al. 2019). These methods will merge features representing different activities together and fail to generate representative features for multi-label activities, as mentioned earlier.

Attention Modules. The attention mechanism was introduced for capturing long-range associations within sequential inputs, which is commonly used in the natural language processing tasks (Bahdanau, Cho, and Bengio 2014; Vaswani et al. 2017). Existing activity recognition approaches apply spatial attention to aggregate the backbone features (output of the last convolution layer) over space and temporal attention to aggregate the feature maps over time (Li et al. 2018; Meng et al. 2019; Du, Wang, and Qiao 2017; Girdhar and Ramanan 2017). The nonlocal block is an extension of these methods for generating spatio-temporal attention instead of separately using cascade attention in space and time (Wang et al. 2018). However, these methods do not work well on multi-label activities in that all the channels of the feature maps share the same attention, which causes the feature maps to fail to highlight important regions.

Bag-of-Features. Bag-of-words methods were initially developed for document classification and further extended to

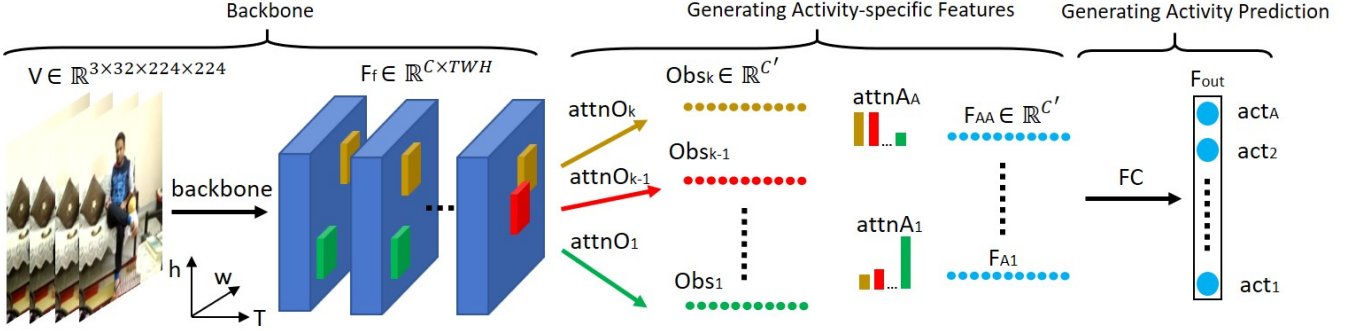


Figure 2: Method overview, showing the detail dimension transformation when generating activity-specific features and providing predictions. Attention (red, green, and brown) focus on different spatio-temporal regions of the backbone feature (F_f) for generating observations (Obs), and generating activity-specific features (F_A) by combining observations using $attnA$.

bag-of-visual-features for image recognition (Csurka et al. 2004; Arandjelovic et al. 2016; Yan, Smith, and Zhang 2017; Sudhakaran and Lanz 2019; Tu et al. 2019; Girdhar et al. 2017). These methods benefit from requiring fewer parameters by encoding large images into visual words. The step that generating activity-specific features in our network is related to the idea of bag-of-features.

Methodology

Inspired by the idea of creating “action words” from the Action-VLAD and other bag-of-features methods (Girdhar et al. 2017; Sudhakaran and Lanz 2019; Tu et al. 2019), we introduce a method that generates independent feature descriptors for each activity (activity-specific features). Compared to the Action-VLAD and other bag-of-features methods, our activity-specific features are end-to-end trainable unlike their visual words that are generated using unsupervised learning methods. In addition, our activity-specific features focus on different spatio-temporal regions instead of aggregating features over time as the Action-VLAD did. Given a video clip $V \in \mathbb{R}^{3 \times 32 \times 224 \times 224}$ with 32 consecutive frames, our model provides activity predictions in two steps:

- 1. Generating activity-specific features:** we generate independent feature representations for A different activities. This step consists of two sub-steps: we first generate K spatio-temporally independent feature snippets (observations), $Obs \in \mathbb{R}^{K \times C'}$, that focus on different spatio-temporal regions of the video (Figure 2, left). We then apply attention $attn_A$ on the observations to generate feature descriptors F_A (activity-specific features) that are independent for each activity using independent weighted combinations of observations (Figure 2, middle).
- 2. Generating activity predictions:** we finally provide prediction for each activity by using its corresponding activity-specific features (Figure 2, right).

Generating Activity-specific Features

Given a feature set $F_f \in \mathbb{R}^{C \times T \times W \times H}$ from the backbone network (e.g., i3D (Carreira and Zisserman 2017)), the activity-specific features can be generated as:

$$F_A = \{attnA_1 Obs, attnA_2 Obs, \dots, attnA_A Obs\} \quad (1)$$

where $F_A \in \mathbb{R}^{A \times C'}$ denotes A independent feature descriptors for their corresponding activities (activity-specific features), C' is the channel number of F_A , $Obs \in \mathbb{R}^{K \times C'}$ denotes K independent feature snippets (observations) that are extracted from the backbone features F_f , and $attnA_i$ ($i \in 1, 2, \dots, A$) are the attentions that independently combine the K observations to generate activity-specific features for the i^{th} activity. We create these observations instead of directly generating $attnA$ from the backbone features F_f to reduce redundant information. Each observation is an independent spatio-temporal feature snippet that focuses on a specific key region in a video. The Obs are generated by applying K independent spatio-temporal attentions on F_f as:

$$Obs_k = attnO_k [g_k^\alpha(F_f)]^T \quad (2)$$

$$Obs = \{Obs_1, Obs_2, \dots, Obs_k\} \quad (3)$$

where $Obs_k \in \mathbb{R}^{C'}$ is the k^{th} observation that focuses on a specific key region of the video, $attnO_k \in \mathbb{R}^{T \times W \times H}$ denotes the spatio-temporal attention for generating the k^{th} observation. The g_k^α is the linear function to integrate channels from F_f , which is represented as:

$$g_k^\alpha(F_f) = W_k^\alpha F_f \quad (4)$$

where $W_k^\alpha \in \mathbb{R}^{C' \times C}$ are the weights for the linear function g_k^α . The activity-specific set F_A can finally be written as:

$$F_A = \{attnA_1 \{attnO_1 [g_1^\alpha(F_f)]^T, \dots, attnO_k [g_k^\alpha(F_f)]^T\} \\ attnA_2 \{attnO_1 [g_1^\alpha(F_f)]^T, \dots, attnO_k [g_k^\alpha(F_f)]^T\} \\ \dots \\ attnA_A \{attnO_1 [g_1^\alpha(F_f)]^T, \dots, attnO_k [g_k^\alpha(F_f)]^T\}\} \quad (5)$$

Generating Attentions The attention mechanism was introduced for capturing long-term dependencies within sequential inputs and is commonly used in nature language processing systems. We applied attentions for generating spatio-temporal independent observations from the backbone features ($attnO$) and generating activity-specific features by combining observations ($attnA$). We implemented the dot-product attention method (Vaswani et al. 2017) for generating $attnO$ as:

$$attnO_k = softmax([g_k^\beta(F_f)_{-1}]^T g_k^\gamma(F_f)) \quad (6)$$



Figure 3: A video example in Charades shows multiple activities (opening a fridge and walking through a doorway) that require inputs with different sample rates.

where $attnO_k \in \mathbb{R}^{TWH}$ denotes the attention for the k^{th} observation, g_k^β, g_k^γ are the linear functions same as the g_k^α in equation 4, and $g_k^\beta(F_f)_{-1} \in \mathbb{R}^{C' \times 1}$ denotes selecting the last row of the $g_k^\beta(F_f) \in \mathbb{R}^{C' \times TWH}$ to produce an appropriate dimension for $attnO_k$. The $attnA$ was generated using a similar approach. Other attention methods (e.g. additive attention (Bahdanau, Cho, and Bengio 2014)) could be used for generating attentions, but we selected the dot-product attention method because previous researches has shown that it is more efficient and works well for machine translation (Vaswani et al. 2017; Shen et al. 2017).

Applying linear functions in equation (4) requires a large number of weights. To reduce the number of weights for g_k^α , we used a group 1D convolution to simulate the linear function in equation (4) as:

$$g_k^\alpha(F_f) = conv1d(F_f, group = n) \quad (7)$$

Using a larger number of groups (n) results in fewer parameters. We set $n = 16$ empirically to minimize the number of weights without affecting the performance of the model.

Generating Activity Predictions

The final step of the module is to predict activities using those activity-specific features as:

$$F_{out} = sigmoid(W^\varphi F_A + b^\varphi) \quad (8)$$

where $F_{out} \in \mathbb{R}^{A \times 1}$ is the output of the model. W^φ and b^φ are the trainable weights and bias for decoding the activity-specific features F_A into the binary predictions. We compared the model performance by using independent fully-connected layers for each activity and a shared fully-connected layer for decoding all the activities from their corresponding activity-specific features. The two methods achieved similar performance. We choose to apply a shared fully-connected layer to reduce the number of parameters.

Comparison with Other Attention Methods

Attention-based module with spatial and temporal attentions has already been used for activity recognition to extract features by focusing on important spatio-temporal regions (Girdhar and Ramanan 2017; Du, Wang, and Qiao 2017; Li et al. 2018; Meng et al. 2019; Girdhar and Ramanan 2017). The nonlocal neural network extends from them that generates spatio-temporal attention instead of separately using

cascade attention in space and time (Wang et al. 2018). However, both the nonlocal and other attention-based approaches make all the channels in F_f share the same attention. These methods do not work well for multi-label activities because the feature maps from different channels of the backbone features F_f may focus on different regions that correspond to different activities. Using shared attention through channels would cause feature maps to focus on irrelevant regions that might contain information important in the feature maps of other channels. In our approach, ‘‘observations’’ independently focus on different key regions of the video because they are generated by integrating different subsets from the channels of F_f and applying independent spatio-temporal attention on each subset.

Implementation

Implementation Details

We implemented our model with PyTorch (Paszke et al. 2017). We used batch normalization (Ioffe and Szegedy 2015) and ReLU activation (Hahnloser and Seung 2001) for all the convolution layers. We used binary cross-entropy loss and the SGD optimizer with an initial learning rate $3.5e - 2$ and $1.25e - 5$ as the weight decay. Dropout (rate=0.5) was used after the dense layer to avoid overfitting (Srivastava et al. 2014). We set the batch size to 9 and trained our model with 3 RTX 2080 Ti GPUs for 50k iterations.

We applied spatio-temporal augmentation to avoid overfitting. We applied the scale-jittering method in the range of [256, 320] and horizontal flipping to augment the frames in spatial ((Feichtenhofer et al. 2019)). Temporally, we randomly picked a starting point in the video and selected the consecutive 32 frames. For the short videos having less than 32 frames, we padded the videos at the end by duplicating the last frame from the video.

Speed-invariant Tuning

Algorithm 1: Speed-invariant Tuning

- 1 Train the entire model with the video sampling rate to s ;
 - 2 Freeze the backbone network (3D-Conv layers) weights;
 - 3 **for** $iteration=0, I$ **do**
 - 4 Randomly select a sample rate $r \in (\frac{s}{2}, s, 2s)$;
 - 5 Fetch consecutive frames from the video downsampled by r and gain its corresponding ground truth y ;
 - 6 Perform a gradient step on $y - F_{out}$ according to equation (8);
 - 7 **end**
 - 8 Evaluate the model on testing set with video level predictions generated by summing predictions using all the sample rate $r \in (\frac{s}{2}, s, 2s)$;
-

In multi-label activity videos, different activities may have different duration. Figure 3 shows an example in Charades having two activities, opening a fridge and walking through a doorway. Because our system requires the same number of frames (32) for each input clip, using the same sampling rate for video frames may cover long activities only partially and short activities may appear in only a few

Table 1: Charades evaluation using mAP (mean-average-precision) in percentages, calculated using the officially provided script. The Charades ego means using Charade ego dataset as supplemental.

method	backbone	mAP
2D CNN (Sigurdsson et al. 2016)	Alexnet	11.2
2-stream (Sigurdsson et al. 2016)	VGG16	22.4
Action-VLAD (Girdhar et al. 2017)	VGG16	21.0
CoViAR (Wu et al. 2018)	Res2D-50	21.9
MultiScale TRN (Zhou et al. 2018)	Inception	25.2
I3D (Carreira and Zisserman 2017)	Inception	32.9
STRG (Wang and Gupta 2018)	Nonlocal-101	39.7
LFB (Wu et al. 2019)	Nonlocal-101	42.5
SlowFast (Feichtenhofer et al. 2019)	SlowFast-101	45.2
Multi-Grid (Wu et al. 2020)	SlowFast-50	38.2
X3D (Feichtenhofer 2020)	X3D	47.2
CSN (Tran et al. 2019) (Baseline)	CSN-152	45.4
Our's	CSN-152	48.2
Our's + Charades ego	CSN-152	50.3

frames. To ensure that activities of different duration are properly covered in 32-frame inputs we introduced a speed-invariant tuning method. We first trained the complete model using the downsampling rate of 4 and froze the weights for all the 3D convolution layers (Algorithm 1, step 1-2). We then started finetuning the module after the 3D convolution for I iterations by using 32-frame inputs obtained by randomly selecting downsampling rate r among 2, 4, and 8 (Algorithm 1, step 3-7). During the testing stage, we summed the predictions of the model that were generated based on all three downsampling rates $r \in \{2, 4, 8\}$ for the final video-level activity prediction (Algorithm 1, step 8). The full algorithm of our speed-invariant tuning method is presented in Algorithm 1. We set the initial sampling rate s to 4 as in (Wang et al. 2018). The model can then recognize activities that have different duration by aggregating the results from branches that used different downsampling rate as the input.

Experiments

We evaluated our method on three multi-label activity datasets: one large-scale dataset, Charades (Sigurdsson et al. 2016), and two small datasets, Volleyball (Sozykin et al. 2018) and Hockey (Carbonneau et al. 2015). To show that our proposed method generalizes to different activity recognition tasks, we also tested it on Kinetics-400 (Kay et al. 2017) and UCF-101 (Soomro, Zamir, and Shah 2012), two commonly used single-activity recognition datasets.

Experiments on Charades

Charades dataset (Sigurdsson et al. 2016) contains 9848 videos with average length of 30 seconds. This dataset includes 157 multi-label daily indoor activities. We used the officially provided train-validate split (7985/1863). We used the officially-provided 24-fps RGB frames as input and the officially-provided evaluation script for evaluating the validation set. During the evaluation, we used the 30-view test followed (Feichtenhofer et al. 2019).

Results Overview on Charades We compared our system with the baseline network, CSN (Tran et al. 2019),

pre-trained on IG-65M (Ghadiyaram, Tran, and Mahajan 2019)), as well as other state-of-the-art methods that work on Charades. Compared to the baseline network, our method achieved around 3% higher mAP score on Charades. We outperformed all the other methods (Wu et al. 2019; Hussein, Gavves, and Smeulders 2019; Wang and Gupta 2018; Feichtenhofer et al. 2019) and the recent state-of-the-art approach, X3D (Feichtenhofer 2020) that pre-trained on Kinetics-600 (Carreira et al. 2018) on Charades. This shows that our activity-specific features are representative of their corresponding activities and works better for multi-label activity recognition tasks. Because the model performance on Charades highly depends on the pre-trained backbone network, our method could be further improved if we could use the most recent X3D as backbone (Feichtenhofer 2020).

Our method significantly outperformed another bag-of-features method Action-VLAD on Charades (48.2% vs. 21.0%) because our network captures spatio-temporal features independently for each activity, instead of aggregating the visual-words over time. In addition, Action-VLAD only works on 2D backbone networks, which cannot benefit from the recent 3D backbone networks that work better for activity recognition.

Charades is relatively small for recognizing more than 100 multi-label activities. To further boost the performance of our model on Charades, we included the videos from the Charades Ego dataset (Sigurdsson et al. 2018) into the training set. Charades Ego dataset (Sigurdsson et al. 2018) contains 3930 videos having the same activity list as Charades. There are no overlapping videos between these two datasets. Our model after including the Charades Ego achieved 50.3% mAP on Charades.

Ablation Experiment on Charades We next ablated our system with various hyper-parameters (group size, observation number, and sampling rate for speed-invariant inputs).

Group sizes. Table 2a shows the system performance for different values of the group size (n) in equation 7 when generating observations (the number of observations is 64 and the downsampling rate is 4). The performance on Charades stayed at 47% when the group size increased from 1 to 16 but dropped quickly for $n = 32$. A larger group size results in using a smaller subset of channels from F_f for generating observations, which requires fewer parameters but may cause performance drop because of information loss.

Observations number. Table 2b compares the system performance for different number of observations (group size is 16 and the downsampling rate is 4). The best-performing number of observations is 64, which also requires fewest weights. Using a larger number of observations helps cover more key parts from the videos but the performance saturates when for more than 64 observations.

Model structure ablation. We then evaluated the system on Charades by removing each component from our network. The model without $attn_A$ is implemented by flattening the dimensions of observations and feature channels, and recognizing activities using a fully-connected layer. Table 2c shows that the model without $attn_A$ for generating activity-specific features achieved similar performance as the base-

Table 2: Ablation experiments on the Charades dataset. We show the mAP scores and parameter numbers by using different hyper-parameters, backbone networks, and removing different modalities from our tri-axial attention module.

group size	mAP	# Params	obs num	mAP	# Params	model structures	mAP
1	46.9	50.4M	16	45.9	0.8M	baseline	45.4
8	47.0	6.3M	32	46.2	1.6M	no $attn_O$	-
16	47.1	3.2M	64	47.1	3.2M	no $attn_A$	46.5
32	46.3	1.6M	128	46.7	6.3M	complete	47.1

(a) Group size: performance on Charades when using different group sizes by setting observation number to 64 and sample rate to 4.

(b) Observation number: performance on Charades when using different number of observations by setting group size to 16 and sample rate to 4.

(c) Model structure ablation: performance on Charades after removing each processing stage from the tri-axial attention.

sample rate	mAP	# Params
4 only	47.1	1 ×
2 + 4	47.9	1 ×
2 + 4 + 8	48.2	1 ×

(d) Sample rate for speed-invariant tuning: performance on Charades when using different sample rates by setting observation number to 64 and group size to 16.

method	Backbone	mAP
Baseline/ Ours	Nonlocal-50	38.3/ 40.8
Baseline/ Ours	Nonlocal-101	40.3/ 43.5
Baseline/ Ours	CSN-152	45.4/ 48.2

(e) Backbone network: performance on Charades by plugging into different baseline models.

line model, because the fully-connected layer applied on a flattened feature vector requires a large number of weights, which causes overfitting. The model without $attn_O$ is implemented by setting the observation number K equal to the number of activities A . We failed to get the result for this model on Charades because it caused out-of-memory error due to the huge number of parameters. These results show that our network achieves a performance boost by the combination of key components of our network.

Sampling rates for speed-invariant tuning. We also evaluated our speed-invariant tuning method by merging predictions using different downsampling rates at inputs. Table 2d shows that speed-invariant models achieved better performance compared to the model using a single downsampling rate of 4 because the speed-invariant tuning method makes the features better represent activities of different duration. The system achieved the best performance by merging predictions based on 2, 4, and 8 downsampling rates and this method did not require extra parameters (Table 2d row 3).

Backbone network. We finally evaluated our model by plugging our method in to different backbone networks. Table 2e shows that our method achieved around 2.5% mAP score increase on Charades after being plugged into all the three backbone networks (Nonlocal-50, Nonlocal-101 (Wang et al. 2018), and CSN-152 (Tran et al. 2019)). That shows our method generalized well on multi-label activity recognition by using different existing backbone networks.

Experiments on Hockey and Volleyball

We also run experiments on two small datasets, Hockey and Volleyball (Ibrahim et al. 2016; Sozykin et al. 2018). The Volleyball Dataset contains 55 videos with 4830 annotated video clips. This dataset includes two sets of labels for group activity recognition task (8-class multi-class classification) and multi-label activity recognition task (9-label multi-label classification). We evaluated our method on both of these tasks. **The experimental results on Hockey is in the supplemental material because of the page limit.**

Table 3 shows that our system substantially outperformed all the existing approaches on Volleyball for multi-label

Table 3: Experimental results on Volleyball. The “s” and “bb” in the last two columns denote using the whole scene and bounding boxes of persons as supplemental for recognizing group activities.

method	Volleyball Personal (multi-label)			Volleyball Group		
	Acc.	Acc. (s)	Acc. (bb)	Acc.	Acc. (s)	Acc. (bb)
Hier LSTM (Ibrahim et al. 2016)	72.7	63.1	81.9			
SRNN (Biswas and Gall 2018)	76.6	-	83.4			
So-Sce (Bagautdinov et al. 2017)	82.4	75.5	89.9			
CRM (Azar et al. 2019)	-	75.9	93.0			
Act-trans (Gavrilyuk et al. 2020)	85.9	-	94.4			
CSN-152 baseline	85.0	87.1	-			
Our’s	86.2	87.2	-			
Our’s + speed-invariant	86.6	87.6	95.5			

activities (Gavrilyuk et al. 2020). We also compared our method with the baseline model using the latest backbone network (CSN baseline in Table 3) that works on activity recognition. Our system achieved roughly 2% higher accuracy score compared with the baseline model, which shows that the activity-specific features also improve multi-label activity recognition on small sports datasets.

We further evaluated our method on Volleyball for group activity recognition. The group activity is essentially a single-activity recognition problem: only one activity occurs during one video clip. Our method outperformed other state-of-the-art methods when using the whole scene (s) as input (Gavrilyuk et al. 2020) (RGB frames without using bounding boxes around people). This shows that our method generalizes for the single-activity recognition problem as well. Previous methods (Azar et al. 2019; Gavrilyuk et al. 2020) used bounding boxes around people (bb) and their individual activities as supplemental information for group activity recognition. We tested our model by including this supplemental information, and our approach outperformed the recent state-of-the-art method (Azar et al. 2019) (95.5 for our system vs. 94.4 for the Act-trans in the last column of Table 3). Compared to the baseline network, our method slightly outperformed the baseline network (87.2 vs. 87.1 in the second-to-the-last column of Table 3). The activity-specific features do not help significantly in the single-activity problems, unlike the case of multi-label activities,

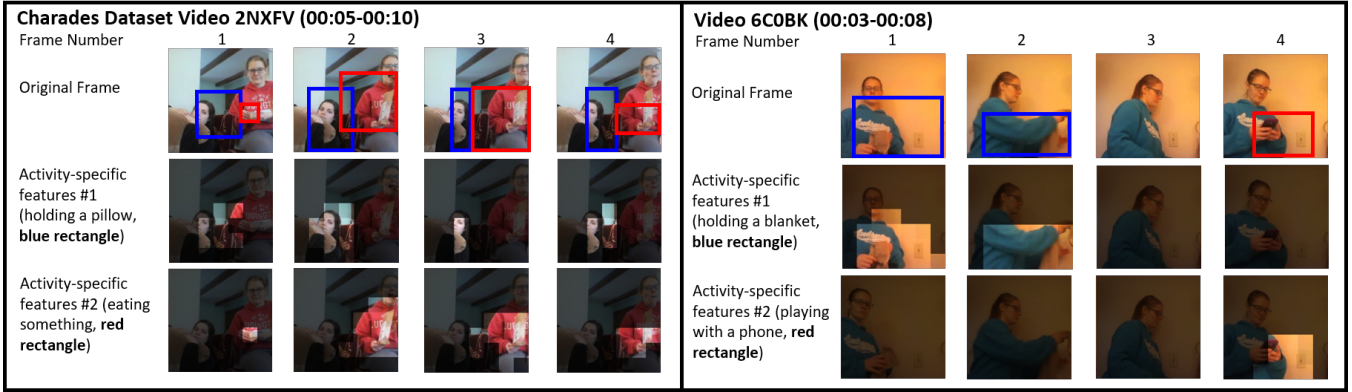


Figure 4: Visualizing the activity-specific features in two videos from the Charades dataset. The bounding boxes in the original frames correspond to the activated regions in the activity-specific feature maps. The activity-specific feature maps will only focus on the regions where corresponding activities are being performed and have low values if there is no activity being performed at that time.

Table 4: Method evaluation on Kinetics-400 and UCF-101. The scores are top1 accuracy in percentage.

method	flow	K400	ucf-101
I3D (Carreira and Zisserman 2017)	×	72.1	95.4
TSM (Lin, Gan, and Han 2018)	✓	74.1	95.9
R(2+1)D (Tran et al. 2018)	✓	73.9	97.3
S3D (Xie et al. 2018)	✓	77.2	78.8
SlowFast (Feichtenhofer et al. 2019)	×	79.8	-
TPN (Yang et al. 2020)	×	78.9	-
X3D (Feichtenhofer 2020)	×	80.4	-
CSN baseline (Tran et al. 2019)	×	82.6	97.1
Our's	×	82.7	97.3

because the feature maps will only focus on one region where the single-activity occurred.

Experiment on Kinetics-400 and UCF-101

To demonstrate that our method is generalizable for single-activity recognition tasks, we evaluated our method on two single-activity recognition datasets, Kinetics-400 (Kay et al. 2017) and UCF-101 (Soomro, Zamir, and Shah 2012). We fine-tuned our network with the backbone weights frozen. Table 4 shows that our approach, although specialized for multi-label activity recognition, generalized well for single-activity datasets and achieved similar results as the current state-of-the-art approaches (bottom row in Table 4). Our method slightly outperformed the baseline network (CSN baseline in Table 4) because both the datasets contain only single-activities. As we described earlier, activity-specific features do not help significantly for single-activities.

Feature Visualization

To better understand what activity-specific features are learned, we visualized these features for the activities present in the video clips. Figure 4 shows two examples in the Charades, including the activity-specific feature maps (last two rows of each example in Figure 4) and their corresponding input frames. The activity-specific feature maps were generated by applying the learned $attn_O$ and $attn_A$ on the backbone features F_f . We normalized the feature maps between 0 and 1 and plotted these maps for the activities present in the video (last two rows of each example in Figure 4). To make the visualized maps more understandable, we

applied the 0.5 threshold to the activity-specific feature maps and drew the bounding boxes using different colors (blue, red) for different activities in the original frames around the regions activated in the feature maps.

Based on the visualizations in Figure 4, we can make three points. First, the activity-specific features will only focus on the spatial regions for the corresponding activity when multiple activities are performed simultaneously. The visualization of video “2NXFV” (Figure 4, left) shows the activity-specific features #1 (holding a pillow) focusing the region of the left person, and activity-specific features #2 (eating something) focusing the right person who is performing the corresponding activity. Second, only the activity-specific features corresponding to the activity being performed will have high values when the video has one activity or activities performed in sequence. The visualization of video “6C0BK” (Figure 4, right) shows the activity-specific features #1 (holding a blanket) having activated regions at the first two frames, while the activity-specific features #2 (playing with a phone) focused on the last frames. Finally, all the activity-specific features will have low values for the frames in which no activities were performed (Figure 4, the third column of the right diagram). These visualizations demonstrate that the activity-specific features will focus on the key regions from the video that are related to their corresponding activities.

Conclusion and Future Work

We introduced a novel network that focuses on multi-label activity recognition. The system generates spatio-temporally independent activity-specific features for each activity and outperformed previous state-of-the-art methods on three multi-label activity recognition datasets. The visualizations showed that the activity-specific features are representative of their corresponding activities. We also evaluated our method on two single-activity recognition datasets to show the generalizability of our method. One issue remains in the speed-invariant tuning method, where we simply summed the predictions by using different downsampling rates for the inputs. Extending the speed-invariant method to enable the model to learn to select features from appropriate scales for different activities will be our future work.

References

- Arandjelovic, R.; Gronat, P.; Torii, A.; Pajdla, T.; and Sivic, J. 2016. NetVLAD: CNN architecture for weakly supervised place recognition. In *Proceedings of the IEEE conference on computer vision and pattern recognition*, 5297–5307.
- Azar, S. M.; Atigh, M. G.; Nickabadi, A.; and Alahi, A. 2019. Convolutional Relational Machine for Group Activity Recognition. In *Proceedings of the IEEE Conference on Computer Vision and Pattern Recognition*, 7892–7901.
- Bagautdinov, T.; Alahi, A.; Fleuret, F.; Fua, P.; and Savarese, S. 2017. Social scene understanding: End-to-end multi-person action localization and collective activity recognition. In *Proceedings of the IEEE Conference on Computer Vision and Pattern Recognition*, 4315–4324.
- Bahdanau, D.; Cho, K.; and Bengio, Y. 2014. Neural machine translation by jointly learning to align and translate. *arXiv preprint arXiv:1409.0473*.
- Biswas, S.; and Gall, J. 2018. Structural recurrent neural network (srnn) for group activity analysis. In *2018 IEEE Winter Conference on Applications of Computer Vision (WACV)*, 1625–1632. IEEE.
- Carbonneau, M.-A.; Raymond, A. J.; Granger, E.; and Gagnon, G. 2015. Real-time visual play-break detection in sport events using a context descriptor. In *2015 IEEE International Symposium on Circuits and Systems (ISCAS)*, 2808–2811. IEEE.
- Carreira, J.; Noland, E.; Banki-Horvath, A.; Hillier, C.; and Zisserman, A. 2018. A short note about kinetics-600. *arXiv preprint arXiv:1808.01340*.
- Carreira, J.; and Zisserman, A. 2017. Quo vadis, action recognition? a new model and the kinetics dataset. In *proceedings of the IEEE Conference on Computer Vision and Pattern Recognition*, 6299–6308.
- Csurka, G.; Dance, C.; Fan, L.; Willamowski, J.; and Bray, C. 2004. Visual categorization with bags of keypoints. In *Workshop on statistical learning in computer vision, ECCV*, volume 1, 1–2. Prague.
- Du, W.; Wang, Y.; and Qiao, Y. 2017. Recurrent spatial-temporal attention network for action recognition in videos. *IEEE Transactions on Image Processing* 27(3): 1347–1360.
- Feichtenhofer, C. 2020. X3D: Expanding Architectures for Efficient Video Recognition. In *Proceedings of the IEEE/CVF Conference on Computer Vision and Pattern Recognition*, 203–213.
- Feichtenhofer, C.; Fan, H.; Malik, J.; and He, K. 2019. Slow-fast networks for video recognition. In *Proceedings of the IEEE international conference on computer vision*, 6202–6211.
- Feichtenhofer, C.; Pinz, A.; and Zisserman, A. 2016. Convolutional two-stream network fusion for video action recognition. In *Proceedings of the IEEE conference on computer vision and pattern recognition*, 1933–1941.
- Gavrilyuk, K.; Sanford, R.; Javan, M.; and Snoek, C. G. 2020. Actor-transformers for group activity recognition. *arXiv preprint arXiv:2003.12737*.
- Ghadiyaram, D.; Tran, D.; and Mahajan, D. 2019. Large-scale weakly-supervised pre-training for video action recognition. In *Proceedings of the IEEE Conference on Computer Vision and Pattern Recognition*, 12046–12055.
- Girdhar, R.; and Ramanan, D. 2017. Attentional pooling for action recognition. In *Advances in Neural Information Processing Systems*, 34–45.
- Girdhar, R.; Ramanan, D.; Gupta, A.; Sivic, J.; and Russell, B. 2017. Actionvlad: Learning spatio-temporal aggregation for action classification. In *Proceedings of the IEEE Conference on Computer Vision and Pattern Recognition*, 971–980.
- Goyal, R.; Kahou, S. E.; Michalski, V.; Materzynska, J.; Westphal, S.; Kim, H.; Haenel, V.; Freund, I.; Yianilos, P.; Mueller-Freitag, M.; et al. 2017. The “Something Something” Video Database for Learning and Evaluating Visual Common Sense. In *ICCV*, volume 1, 3.
- Hahnloser, R. H.; and Seung, H. S. 2001. Permitted and forbidden sets in symmetric threshold-linear networks. In *Advances in neural information processing systems*, 217–223.
- He, K.; Zhang, X.; Ren, S.; and Sun, J. 2016. Deep residual learning for image recognition. In *Proceedings of the IEEE conference on computer vision and pattern recognition*, 770–778.
- Hussein, N.; Gavves, E.; and Smeulders, A. W. 2019. Time-ception for Complex Action Recognition. In *Proceedings of the IEEE Conference on Computer Vision and Pattern Recognition*, 254–263.
- Ibrahim, M. S.; Muralidharan, S.; Deng, Z.; Vahdat, A.; and Mori, G. 2016. A hierarchical deep temporal model for group activity recognition. In *Proceedings of the IEEE Conference on Computer Vision and Pattern Recognition*, 1971–1980.
- Ioffe, S.; and Szegedy, C. 2015. Batch normalization: Accelerating deep network training by reducing internal covariate shift. *arXiv preprint arXiv:1502.03167*.
- Kay, W.; Carreira, J.; Simonyan, K.; Zhang, B.; Hillier, C.; Vijayanarasimhan, S.; Viola, F.; Green, T.; Back, T.; Natsev, P.; et al. 2017. The kinetics human action video dataset. *arXiv preprint arXiv:1705.06950*.
- Krizhevsky, A.; Sutskever, I.; and Hinton, G. E. 2012. ImageNet classification with deep convolutional neural networks. In *Advances in neural information processing systems*, 1097–1105.
- Kuehne, H.; Jhuang, H.; Garrote, E.; Poggio, T.; and Serre, T. 2011. HMDB: a large video database for human motion recognition. In *2011 International Conference on Computer Vision*, 2556–2563. IEEE.
- Li, D.; Yao, T.; Duan, L.-Y.; Mei, T.; and Rui, Y. 2018. Unified spatio-temporal attention networks for action recognition in videos. *IEEE Transactions on Multimedia* 21(2): 416–428.
- Li, X.; Zhang, Y.; Zhang, J.; Chen, S.; Marsic, I.; Farneth, R. A.; and Burd, R. S. 2017. Concurrent activity recognition with multimodal CNN-LSTM structure. *arXiv preprint arXiv:1702.01638*.

- Lin, J.; Gan, C.; and Han, S. 2018. Temporal shift module for efficient video understanding. *arXiv preprint arXiv:1811.08383*.
- Meng, L.; Zhao, B.; Chang, B.; Huang, G.; Sun, W.; Tung, F.; and Sigal, L. 2019. Interpretable spatio-temporal attention for video action recognition. In *Proceedings of the IEEE International Conference on Computer Vision Workshops*, 0–0.
- Paszke, A.; Gross, S.; Chintala, S.; Chanan, G.; Yang, E.; DeVito, Z.; Lin, Z.; Desmaison, A.; Antiga, L.; and Lerer, A. 2017. Automatic differentiation in PyTorch.
- Shen, T.; Zhou, T.; Long, G.; Jiang, J.; Pan, S.; and Zhang, C. 2017. Disan: Directional self-attention network for rnn/cnn-free language understanding. *arXiv preprint arXiv:1709.04696*.
- Sigurdsson, G. A.; Gupta, A.; Schmid, C.; Farhadi, A.; and Alahari, K. 2018. Actor and observer: Joint modeling of first and third-person videos. In *Proceedings of the IEEE Conference on Computer Vision and Pattern Recognition*, 7396–7404.
- Sigurdsson, G. A.; Varol, G.; Wang, X.; Farhadi, A.; Laptev, I.; and Gupta, A. 2016. Hollywood in homes: Crowdsourcing data collection for activity understanding. In *European Conference on Computer Vision*, 510–526. Springer.
- Simonyan, K.; and Zisserman, A. 2014. Two-stream convolutional networks for action recognition in videos. In *Advances in neural information processing systems*, 568–576.
- Soomro, K.; Zamir, A. R.; and Shah, M. 2012. UCF101: A dataset of 101 human actions classes from videos in the wild. *arXiv preprint arXiv:1212.0402*.
- Sozykin, K.; Protasov, S.; Khan, A.; Hussain, R.; and Lee, J. 2018. Multi-label class-imbalanced action recognition in hockey videos via 3d convolutional neural networks. In *2018 19th IEEE/ACIS International Conference on Software Engineering, Artificial Intelligence, Networking and Parallel/Distributed Computing (SNPD)*, 146–151. IEEE.
- Srivastava, N.; Hinton, G.; Krizhevsky, A.; Sutskever, I.; and Salakhutdinov, R. 2014. Dropout: a simple way to prevent neural networks from overfitting. *The journal of machine learning research* 15(1): 1929–1958.
- Sudhakaran, S.; and Lanz, O. 2019. Top-down attention recurrent vlad encoding for action recognition in videos. *Intelligenza Artificiale* 13(1): 107–118.
- Szegedy, C.; Liu, W.; Jia, Y.; Sermanet, P.; Reed, S.; Anguelov, D.; Erhan, D.; Vanhoucke, V.; and Rabinovich, A. 2015. Going deeper with convolutions. In *Proceedings of the IEEE conference on computer vision and pattern recognition*, 1–9.
- Tran, D.; Bourdev, L.; Fergus, R.; Torresani, L.; and Paluri, M. 2015. Learning spatiotemporal features with 3d convolutional networks. In *Proceedings of the IEEE international conference on computer vision*, 4489–4497.
- Tran, D.; Wang, H.; Torresani, L.; and Feiszli, M. 2019. Video classification with channel-separated convolutional networks. In *Proceedings of the IEEE International Conference on Computer Vision*, 5552–5561.
- Tran, D.; Wang, H.; Torresani, L.; Ray, J.; LeCun, Y.; and Paluri, M. 2018. A closer look at spatiotemporal convolutions for action recognition. In *Proceedings of the IEEE conference on Computer Vision and Pattern Recognition*, 6450–6459.
- Tu, Z.; Li, H.; Zhang, D.; Dauwels, J.; Li, B.; and Yuan, J. 2019. Action-stage emphasized spatiotemporal vlad for video action recognition. *IEEE Transactions on Image Processing* 28(6): 2799–2812.
- Vaswani, A.; Shazeer, N.; Parmar, N.; Uszkoreit, J.; Jones, L.; Gomez, A. N.; Kaiser, Ł.; and Polosukhin, I. 2017. Attention is all you need. In *Advances in neural information processing systems*, 5998–6008.
- Wang, L.; Xiong, Y.; Wang, Z.; Qiao, Y.; Lin, D.; Tang, X.; and Van Gool, L. 2016. Temporal segment networks: Towards good practices for deep action recognition. In *European conference on computer vision*, 20–36. Springer.
- Wang, X.; Girshick, R.; Gupta, A.; and He, K. 2018. Non-local neural networks. In *Proceedings of the IEEE Conference on Computer Vision and Pattern Recognition*, 7794–7803.
- Wang, X.; and Gupta, A. 2018. Videos as space-time region graphs. In *Proceedings of the European Conference on Computer Vision (ECCV)*, 399–417.
- Wu, C.-Y.; Feichtenhofer, C.; Fan, H.; He, K.; Krahenbuhl, P.; and Girshick, R. 2019. Long-term feature banks for detailed video understanding. In *Proceedings of the IEEE Conference on Computer Vision and Pattern Recognition*, 284–293.
- Wu, C.-Y.; Girshick, R.; He, K.; Feichtenhofer, C.; and Krahenbuhl, P. 2020. A Multigrid Method for Efficiently Training Video Models. In *Proceedings of the IEEE/CVF Conference on Computer Vision and Pattern Recognition*, 153–162.
- Wu, C.-Y.; Zaheer, M.; Hu, H.; Manmatha, R.; Smola, A. J.; and Krähenbühl, P. 2018. Compressed video action recognition. In *Proceedings of the IEEE Conference on Computer Vision and Pattern Recognition*, 6026–6035.
- Xie, S.; Sun, C.; Huang, J.; Tu, Z.; and Murphy, K. 2018. Rethinking spatiotemporal feature learning: Speed-accuracy trade-offs in video classification. In *Proceedings of the European Conference on Computer Vision (ECCV)*, 305–321.
- Yan, S.; Smith, J. S.; and Zhang, B. 2017. Action recognition from still images based on deep vlad spatial pyramids. *Signal Processing: Image Communication* 54: 118–129.
- Yang, C.; Xu, Y.; Shi, J.; Dai, B.; and Zhou, B. 2020. Temporal pyramid network for action recognition. In *Proceedings of the IEEE/CVF Conference on Computer Vision and Pattern Recognition*, 591–600.
- Zhou, B.; Andonian, A.; Oliva, A.; and Torralba, A. 2018. Temporal relational reasoning in videos. In *Proceedings of the European Conference on Computer Vision (ECCV)*, 803–818.